J Mater Sci: Mater Med (2010) 21:887–892
DOI 10.1007/s10856-009-3934-7

Positively charged calcium phosphate/polymer nanoparticles for photodynamic therapy

J. Klesing · A. Wiehe · B. Gitter · S. Gräfe · M. Epple

Received: 28 June 2009 / Accepted: 4 November 2009 / Published online: 19 November 2009

Abstract The charge of nanoparticles influences their ability to pass through the cellular membrane, and a positive charge should be beneficial. The negative charge of calcium phosphate nanoparticles with an inner shell of carboxymethyl cellulose (CMC) was reversed by adding an outer shell of poly(ethyleneimine) (PEI) into which the photoactive dye 5,10,15,20-tetrakis(3-hydroxyphenyl)-porphyrin (*m*THPP) was loaded. The aqueous dispersion of the nanoparticles was used for photodynamic therapy with HT29 cells (human colon adenocarcinoma cells), HIG-82 cells (rabbit synoviocytes), and J774A.1 cells (murine macrophages). A high photodynamic activity (killing) together with a very low dark toxicity was observed for HIG-82 and for J774.1 cells at 2 μM dye concentration. The killing efficiency was equivalent to the pure photoactive dye that, however, needs to be administered in alcoholic solution.

1 Introduction

Photodynamic therapy is a clinical method for the treatment of malignant tissues (e.g., tumors) and biofilms. It is based on the administration of photoactive dyes which are then irradiated, typically with a laser. The excited dye leads to the formation of singlet oxygen inside the target cells which then destroys the malignant cells or bacteria [1–6]. An ongoing problem in photodynamic therapy is the delivery of the dye into the host tissue [7]. Typically, the dyes are not water-soluble and must be applied as alcoholic solution which is painful for the patient. Furthermore, the biodegradation of hydrophobic dyes is usually slow [8]. Therefore, alternative delivery systems have been developed, e.g., liposomes [7, 9], polymeric nanoparticles [7], metallic nanoparticles [10, 11], and silica nanoparticles [12, 13].

We have recently presented calcium phosphate nanoparticles with a polymeric shell that incorporates a photoactive dye [14]. Calcium phosphate has the advantage that it occurs as biomineral in mammals (bone and teeth; [15]) and that nanoparticles of calcium phosphate can be easily functionalized with polymers [16, 17]. Here we present positively charged nanoparticles consisting of a calcium phosphate core with shells of carboxymethyl cellulose (anionic) and poly(ethyleneimine) (cationic). Both layers contained the photoactive dye 5,10,15,20-tetrakis(3-hydroxyphenyl)-porphyrin (*m*THPP) which allowed a high loading with the dye.

2 Materials and methods

2.1 Chemicals

The following polymers were used: Carboxymethyl cellulose, CMC (anionic; Aldrich, molecular weight 90,000 g mol^{-1}; degree of substitution, D.S., 0.7), and branched poly(ethyleneimine), PEI (cationic; Aldrich, molecular weight 25,000 g mol^{-1}). Ultrapure water (Purelab ultra instrument from ELGA) was used for all preparations. Calcium lactate (p.a.) and diammonium hydrogenphosphate (p.a.) from Fluka were used. *m*THPP was synthesized

J. Klesing · M. Epple (✉)
Inorganic Chemistry and Center for Nanointegration Duisburg-Essen (CeNIDE), University of Duisburg-Essen, Universitaetsstr. 5-7, 45117 Essen, Germany
e-mail: matthias.epple@uni-due.de

A. Wiehe · B. Gitter · S. Gräfe
biolitec AG, Winzerlaer Str. 2, 07745 Jena, Germany

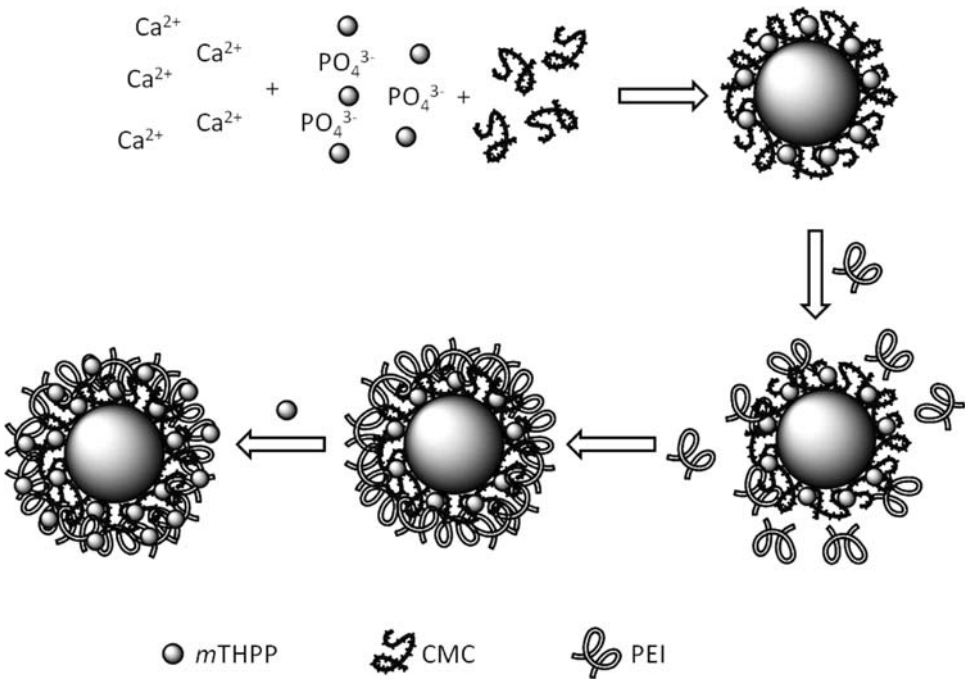

Fig. 1 Schematic view of the preparation of the nanoparticles. A calcium salt, a phosphate salt, *m*THPP molecules, and carboxymethyl cellulose (CMC) were brought together to form a negatively charged particle with *m*THPP (*grey dots*) within the polymer shell. Next, the charge was reversed by the addition of poly(ethyleneimine) (PEI). Finally, further *m*THPP molecules were electrostatically bound to the surface of the particle, resulting in a high loading with *m*THPP

according to a literature procedure [18]. The pathway for the preparation of the nanoparticles is depicted in Fig. 1.

2.2 Preparation of anionic CaP/CMC/mTHPP nanoparticles

CMC-stabilized calcium phosphate nanoparticles incorporating 5,10,15,20-tetrakis(3-hydroxyphenyl)-porphyrin (mTHPP), CaP/CMC/mTHPP, were prepared as follows: Three aqueous solutions were simultaneously pumped at room temperature into a stirred vessel containing 20 ml of water during one minute: First, aqueous calcium lactate (18 mM); second, aqueous $(NH_4)_2HPO_4$ (10.8 mM) and mTHPP in 2-propanol (1 mg ml^{-1}) in a 5:1 volume ratio; and third, aqueous CMC (2 g l^{-1}). The three volumes were 5, 6, and 5 ml. The CMC coated and stabilized the emerging calcium phosphate nanoparticles. The pH of the calcium and phosphate solutions was previously adjusted to 10 with ammonia solution. The final pH of the colloidal dispersion was between 9.2 and 9.5. 25 ml of the dispersion were taken, and the particles were separated from the counter ions (lactate, NH_4^+, Na^+), excess of dissolved CMC and non-adsorbed *m*THPP by ultracentrifugation at 66,000×*g* for 30 min. The centrifuged nanoparticles were redispersed in 20 ml water, centrifuged and redispersed again to 20 ml. To achieve a sufficient stability of this colloidal system, the dispersion had to be diluted with water to a fivefold original volume after redispersion; otherwise, agglomeration occurred within a few days. The final concentration of nanoparticles in the dispersion was 76 ± 5 mg l^{-1}, containing 42 ± 3 mg l^{-1} calcium phosphate (determined by centrifugation of the nanoparticles, drying at room temperature for 2 days, weighing, and elemental analysis). By UV spectroscopy, the concentration of mTHPP was determined to 7.9 μmol l^{-1}, using a calibration curve.

2.3 Preparation of cationic CaP/CMC/mTHPP/PEI/mTHPP nanoparticles

CMC/PEI-stabilized calcium phosphate nanoparticles incorporating 5,10,15,20-tetrakis(3-hydroxyphenyl)-porphyrin (mTHPP), CaP/CMC/mTHPP/PEI/mTHPP, were prepared as follows: The surface charge of the CaP/CMC/*m*THPP nanoparticles (zeta potential: −26 mV) was reversed by adding a layer of the cationic polyelectrolyte PEI. An aqueous solution of PEI (2 g l^{-1}, pH 10.4) was rapidly added to the particle dispersion in a 1:8 volume ratio. The dispersion was stirred for 2 min and 0.74 μmol *m*THPP dissolved in 2-propanol (1 g l^{-1}) were added. The dispersion was stirred for another 15 min and then stored at room temperature for 12 h. The particles were separated from excess PEI by ultracentrifugation at 66,000×*g* for 30 min. The centrifuged nanoparticles were redispersed in ultrapure water to the initial volume. The particles were stable in dispersion for a few weeks. The final concentration of nanoparticles in the dispersion was 66 ± 5 mg l^{-1}, containing 29 ± 3 mg l^{-1} calcium phosphate (determined as described above). By UV spectroscopy, the concentration of *m*THPP was determined to 14.5 μmol l^{-1}, using a calibration curve.

2.4 Methods

Thermogravimetric analysis (TGA) was carried out with a Netzsch STA 409 PC instrument (dynamic oxygen atmosphere; 50 ml min^{-1}; heating rate 1 K min^{-1}; open alumina crucible). X-ray powder diffraction (XRD) was carried out with a STOE transmission diffractometer STADI P 2003-10 (Cu Kα radiation, $\lambda = 1.54$ Å). Scanning electron microscopy coupled with energy-dispersive X-ray spectroscopy (SEM-EDX) was carried out with an ESEM Quanta 400 FEG instrument (FEI; gold–palladium[80:20]-sputtered samples; EDX detector: S-UTW-Si(Li)). Dynamic light scattering (DLS) and zeta potential determinations were carried out with a Zetasizer nanoseries (Malvern Nano-ZS, laser: $\lambda = 532$ nm) instrument. UV-visible absorption spectra were recorded with a Varian Cary WinUV spectrophotometer in 1 cm quartz cuvettes. The contents of carbon, hydrogen, nitrogen and sulfur were determined by standard combustion analysis with an EA 1110 (CE Instruments) instrument. Calcium was determined by atomic absorption spectroscopy (Thermo Electron Corporation, M-Series AA spectrometer). The orthophosphate content was determined by colorimetry using the molybdenum blue method ($\lambda = 725$ nm).

2.5 Cell tests

Cells were obtained from DSMZ, Braunschweig, Germany or ATCC, USA. The cell tests were carried out with HT29 cells (human colon adenocarcinoma cells), HIG-82 cells (synoviocytes from rabbits), and J774A.1 cells (murine macrophages) according to standard procedures as described in Ref. [14] in full detail. Briefly, the cells were cultivated as a monolayer in DMEM (cc-pro GmbH) supplemented with 10% heat-inactivated fetal calf serum (FCS, cc-pro GmbH), 1% penicillin (10,000 I.U., cc-pro GmbH) and streptomycin (10 mg ml^{-1}, cc-pro GmbH) and incubated with the nanoparticle dispersion for 24 h at 37°C in the dark. Before photosensitization, the cells were washed, incubated with RPMI and 10% FCS without phenol red, and then irradiated at room temperature with a 652 nm diode laser (Ceralas PDT 652, biolitec AG) at a fixed flux of 500 mW cm^{-2} for 50 s. Following the irradiation, the cells were incubated in a humidified incubator (5% CO in air at 37°C) for 24 h until the cell viability assay (XTT assay). The dark toxicity was also assessed for each sample, and each experiment was carried out in parallel in four wells.

In each well, 100 µl of a mixture of RMPI with 10% FCS and nanoparticle dispersion were present. The amount of particles in each well (100 µl) was 1.5 µg for CaP/CMC/*m*THPP/PEI nanoparticles at 3.6 µM *m*THPP, 0.9 µg for CaP/CMC/*m*THPP/PEI/*m*THPP nanoparticles at 2.0 µM *m*THPP, and 4.6 µg for CaP/CMC/mTHPP/PEI/*m*THPP nanoparticles at 10 µM mTHPP.

3 Results and discussion

Calcium phosphate nanoparticles were prepared by rapid precipitation from water and then functionalized with a mixture of the dye *m*THPP and the biocompatible anionic polymer carboxymethyl cellulose (CMC). The negative charge (zeta potential −26 mV) [14] was reversed by the addition of another layer of the cationic polymer poly (ethyleneimine) (PEI) to a zeta potential of +32 mV [14]. Onto this layer, further mTHPP was adsorbed, thereby increasing the dye loading of the particles. The preparation pathway is schematically shown in Fig. 1.

The effective concentration of *m*THPP in the nanoparticles was determined by UV spectroscopy with a calibration curve [14]. The absorption spectrum for the dye-loaded nanoparticles is shown in Fig. 2.

The particles were dispersed in aqueous solution and not agglomerated as dynamic light scattering (DLS) clearly showed (Fig. 3). The addition of the PEI/*m*THPP layer increased the particle diameter from 140 to 200 nm, with a slightly broader size distribution. In comparison to the particles without dye (CaP/CMC/PEI), the particle size did not change (Table 1).

This was confirmed by scanning electron microscopy (SEM) which showed almost spherical particles (Fig. 4). Note that the particle size as determined by SEM was smaller than in dynamic light scattering (DLS) because the polymer shell had collapsed during drying; DLS measures the hydrodynamic radius with the water-swollen polymer shell. Table 1 summarizes all characterization data for the

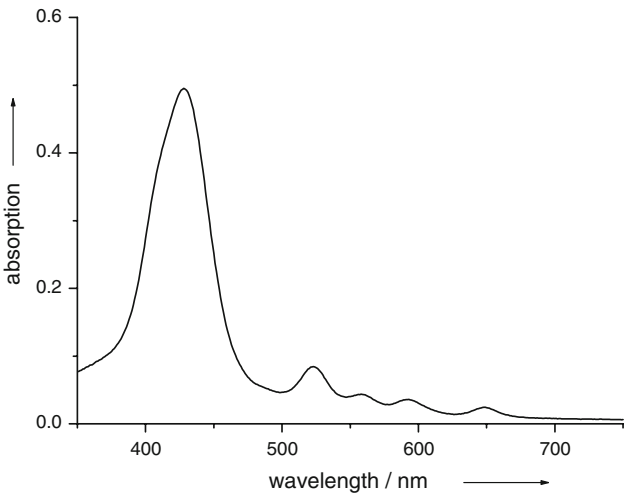

Fig. 2 UV spectrum of CaP/CMC/*m*THPP/PEI/*m*THPP nanoparticles, showing the characteristic absorption bands of the porphyrin dye

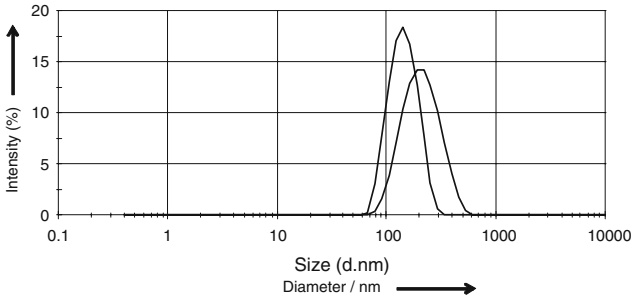

Fig. 3 Dynamic light scattering of the nanoparticles. *Solid line* CaP/CMC/*m*THPP; hydrodynamic diameter 140 nm. *Dashed line* CaP/CMC/*m*THPP/PEI/*m*THPP; hydrodynamic diameter 200 nm

Table 1 Parameters of the prepared nanoparticles, both unloaded and dye-loaded

	CaP/CMC/PEI	CaP/CMC/*m*THPP/PEI/*m*THPP
Diameter (SEM)	80–100 nm	80–100 nm
Diameter (DLS)	200 ± 40 nm	200 ± 40 nm
Polydispersity index (PDI)		
Zeta potential (DLS)	+32 ± 4 mV	+28 ± 4 mV
Ca^{2+}/% (AAS)	22.2 ± 1.0	18.9 ± 1.0
PO_4^{3-}/% (UV)	30.5 ± 1.0	–
C/% (combustion analysis)	12.8 ± 0.3	23.7 ± 0.3
H/% (combustion analysis)	4.2 ± 0.3	4.4 ± 0.3
N/% (combustion analysis)	3.9 ± 0.3	5.6 ± 0.3
Mineral content/% (TG)	65.3 ± 0.5	56.3 ± 0.5
Molar Ca/P ratio	1.73	–
Organic content/% (TG)	25.3 ± 0.5	35.2 ± 0.5
Carbonate content/% (TG)	1.0 ± 0.3	0.8 ± 0.3
Water content/% (TG)	9.4 ± 0.5	8.5 ± 0.5
mTHPP content/% (UV)	0	18.4 ± 0.4

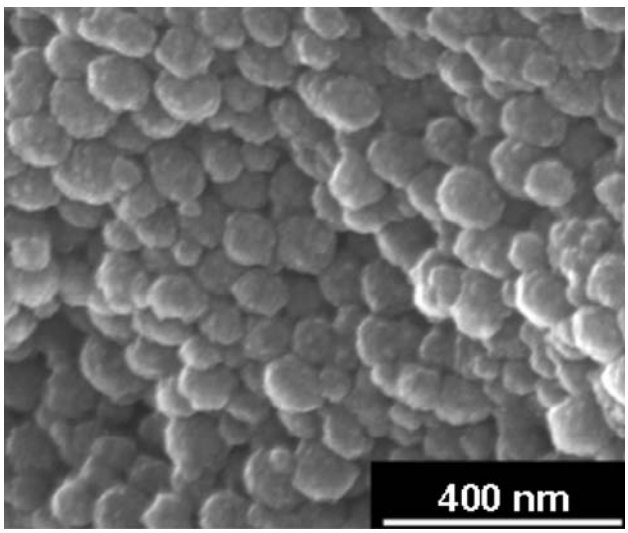

Fig. 4 Scanning electron microscopy of CaP/CMC/*m*THPP/PEI/*m*THPP particles

particles. The charge of the particles was always positive, but the addition of the negatively charged dye *m*THPP led to a small decrease due to electrostatic neutralization (the zeta potential changed from +32 to +28 mV). The particles contained about 55–65 wt% of inorganic material and about 9 wt% water. The organic part of the particles comprised polymer and also *m*THPP in the case of the dye-loaded particles. This was determined by elemental analysis (C,H,N) and also by thermogravimetry. The loading with *m*THPP was 18.4 wt%, i.e., considerably larger than in earlier experiments where the dye was only incorporated into the inner layer of CMC (10.0 wt%) [14].

Cell culture experiments were carried out with three cell lines (Figs. 5, 6 and 7) that represent a range of cell types which are important in photodynamic therapy [14]. As

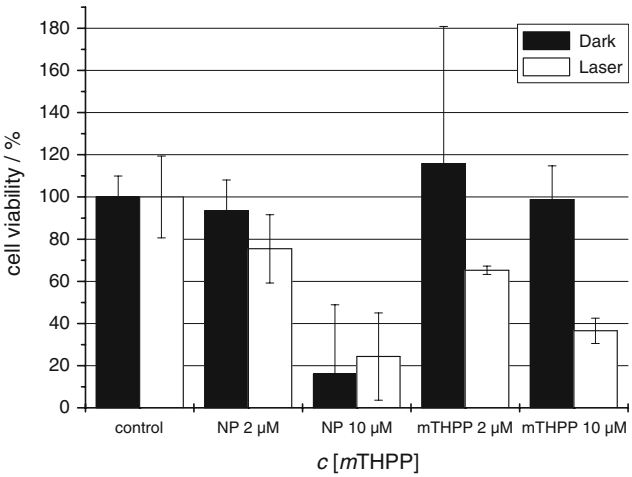

Fig. 5 Results of tests with HT29 cells (adenocarcinoma cells), treated with CaP/CMC/*m*THPP/PEI/*m*THPP nanoparticles (NP) and dissolved dye, respectively

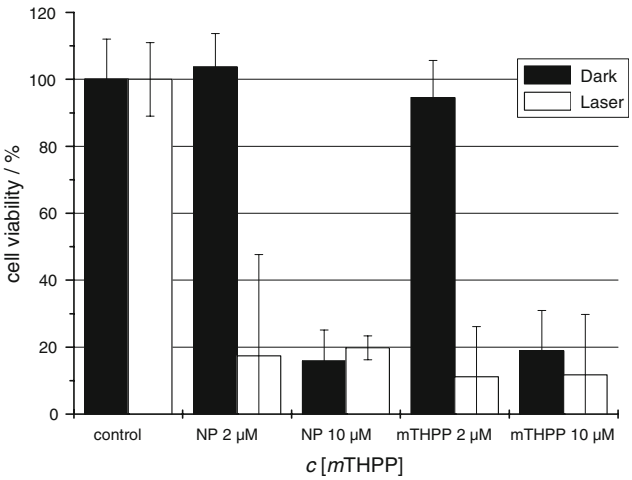

Fig. 6 Results of tests with HIG-82 cells (synoviocytes), treated with CaP/CMC/*m*THPP/PEI/*m*THPP nanoparticles (NP) and dissolved dye, respectively

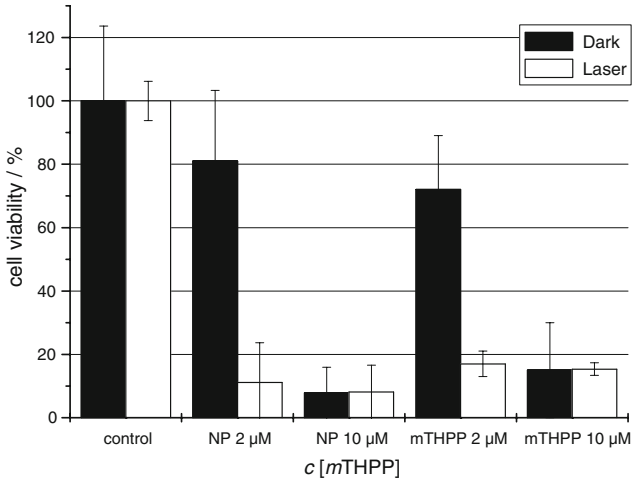

Fig. 7 Results of tests with J774A.1 cells (macrophages), treated with CaP/CMC/*m*THPP/PEI/*m*THPP nanoparticles (NP) and dissolved dye, respectively

comparison, the same concentrations of the pure dye, dissolved in 2-propanol, were always investigated. The control cells were not treated with nanoparticles or dye. With HT29 cells, an efficient killing was not possible. Note that the "killing" is defined as the difference in cell viability between the dark experiment and the laser-irradiated experiment. This confirms earlier results where HT29 cells could not be efficiently treated by photodynamic therapy with similar calcium phosphate nanoparticles [14].

HIG-82 cells showed a good killing at 2 µM, but a high dark toxicity at 10 µM. In comparison to earlier results [14], the dark toxicity was much lower. We ascribe this fact to the lower dose of nanoparticles (0.9 µg vs. 1.5 µg per well) for the new kind of nanoparticles presented here. This reduces the amount of potentially adverse compounds, i.e., poly(ethyleneimine) [19] and calcium [20], which may both be harmful to cells. The dye *m*THPP itself was also toxic at 10 µM in both cases.

Macrophages J774A.1 gave similar results as HIG-82 cells. Again, the experiment at 2 µM dye concentration gave a good killing, and that at 10 µm showed a high toxicity which can be ascribed to the pure dye.

4 Conclusions

Positively charged nanoparticles with a high loading of the photoactive dye were prepared. They showed a good efficiency against HIG-82 and J774A.1 cells. This can be ascribed to the positive charge of the particles (facilitating the transport through the negatively charged cell membrane) and also to the higher loading with the photoactive dye. A smaller amount of nanoparticles is beneficial for cell survival because the amount of potentially harmful PEI and calcium is reduced. Large amounts of calcium phosphate micro- and nanoparticles can lead to a lethal intracellular concentration of calcium [20, 21], although this has not been observed for colloidal dispersions of calcium phosphate nanoparticles [22], probably due to the small concentration. The efficiency was comparable to the pure dye at the same concentration. However, the pure dye must be administered in alcoholic solution which causes pain to the patient. In addition, water-dispersable nanoparticles open the pathway for further surface functionalization to achieve a photodynamic action directed towards specific cell types or bacteria.

Acknowledgments Financial support of this work by the Ministry of Economics, Technology and Labor of Thuringia (grant 2007 FE 0117) is gratefully acknowledged.

References

1. Ackroyd R, Kelty C, Brown N, Reed M. The history of photodetection and photodynamic therapy. Photochem Photobiol. 2001;74:656–69.
2. Bonnett R. Chemical aspects of photodynamic therapy. London: Gordon and Breach; 2000.
3. Castano AP, Mroz P, Hamblin MR. Photodynamic therapy and anti-tumour immunity. Nat Rev Cancer. 2006;6:535–45.
4. Konopka K, Goslinski T. Photodynamic therapy in dentistry. J Dent Res. 2007;86:694–707.
5. MacDonald IJ, Dougherty TJ. Basic principles of photodynamic therapy. J Porphyrins Phtalocyanines. 2001;5:105–29.
6. Maisch T. Anti-microbial photodynamic therapy: useful in the future? Lasers Med Sci. 2007;22:83–91.
7. Konan YN, Gruny R, Allemann E. State of the art in the delivery of photosensitizers for photodynamic therapy. J Photochem Photobiol B. 2002;66:89–106.
8. Ochsner M. Photophysical and photobiological processes in the photodynamic therapy of tumors and non-tumorous diseases. Photochem Photobiol B. 1997;39:1–18.
9. Chen H-K, Hung H-C, Yang TC-K, Wang S-F. The preparation and characterization of transparent nano-sized thermochromic VO_2-SiO_2 films from the sol-gel process. J Non-Cryst Solids. 2004;347:138–43.
10. Cheng Y, Samia AC, Meyers JDP, Panagopoulos I, Fei B, Burda C. Highly efficient drug delivery with gold nanoparticle vectors for in vivo photodynamic therapy of cancer. J Am Chem Soc. 2008;130:10643–7.
11. Hone DC, Walker PI, Evans-Gowing R, FitzGerald S, Beeby A, Chambrier I, et al. Generation of cytotoxic singlet oxygen via phthalocyanine-stabilized gold nanoparticles: a potential delivery vehicle for photodynamic therapy. Langmuir. 2002;18:2985–7.
12. Ohulchanskyy TY, Roy I, Goswami LN, Chen Y, Bergey EJ, Pandey RK, et al. Organically modified silica nanoparticles with covalently incorporated photosensitizer for photodynamic therapy of cancer. Nano Lett. 2007;7:2835–42.
13. Roy I, Ohulchanskyy TY, Pudavar HE, Bergey EJ, Oseroff AR, Morgan J, et al. Ceramic-based nanoparticles entrapping water-insoluble photosensitizing anticancer drugs: a novel drug-carrier system for photodynamic therapy. J Am Chem Soc. 2003;125:7860–5.
14. Schwiertz J, Wiehe A, Graefe S, Gitter B, Epple M. Calcium phosphate nanoparticles as efficient carriers for photodynamic

therapy against cells and bacteria. Biomaterials. 2009;30:3324–31.
15. Dorozhkin SV, Epple M. Biological and medical significance of calcium phosphates. Angew Chem Int Ed. 2002;41:3130–46.
16. Urch H, Franzka S, Dahlhaus D, Hartmann N, Hasselbrink E, Epple M. Preparation of two-dimensionally patterned layers of functionalised calcium phosphate nanoparticles by laser direct writing. J Mater Chem. 2006;16:1798–802.
17. Urch H, Vallet-Regi M, Ruiz L, Gonzalez-Calbet JM, Epple M. Calcium phosphate nanoparticles with adjustable dispersability and crystallinity. J Mater Chem. 2009;19:2166–71.
18. Wiehe A, Shaker YM, Brandt JC, Mebs S, Senge MO. Lead structures for applications in photodynamic therapy. Part 1: synthesis and variation of m-THPC (temoporfin) related amphiphilic A2BC-type porphyrins. Tetrahedron. 2005;61:5535–64.
19. Cai Y, Tang R. Calcium phosphate nanoparticles in biomineralization and biomaterials. J Mater Chem. 2008;18:3775–87.
20. Ewence AE, Bootman M, Roderick HL, Skepper JN, McCarthy G, Epple M, et al. Calcium phosphate crystals induce cell death in human vascular smooth muscle cells—a potential mechanism in atherosclerotic plaque destabilization. Circ Res. 2008;103:28–32.
21. Motskin M, Wright DM, Muller K, Kyle N, Gard TG, Porter AE, et al. Hydroxyapatite nano and microparticles: correlation of particle properties with cytotoxicity and biostability. Biomaterials. 2009;30:3307–17.
22. Neumann S, Kovtun A, Dietzel ID, Epple M, Heumann R. The use of size-defined DNA-functionalized calcium phosphate nanoparticles to minimise intracellular calcium disturbance during transfection. Biomaterials. 2009;30:6794–802.